

Running-Mass Inflation Model and Primordial Black Holes

Manuel Drees^{1, 2 *} and Encieh Erfani^{1, †}

¹*Physikalisches Institut and Bethe Center for Theoretical Physics, Universität Bonn,
Nussallee 12, 53115 Bonn, Germany*

and

²*School of Physics, KIAS, Seoul 130-722, Korea*

Abstract

We revisit the question whether the running-mass inflation model allows the formation of Primordial Black Holes (PBHs) that are sufficiently long-lived to serve as candidates for Dark Matter. We incorporate recent cosmological data, including the WMAP 7-year results. Moreover, we include “the running of the running” of the spectral index of the power spectrum, as well as the renormalization group “running of the running” of the inflaton mass term. Our analysis indicates that formation of sufficiently heavy, and hence long-lived, PBHs still remains possible in this scenario. As a by-product, we show that the additional term in the inflaton potential still does not allow significant negative running of the spectral index.

arXiv:1102.2340v3 [hep-ph] 8 Apr 2011

*drees@th.physik.uni-bonn.de

†erfani@th.physik.uni-bonn.de

1 Introduction

The Cosmic Microwave Background (CMB) is very smooth. Full-sky observations allow to expand the measured CMB temperature in spherical harmonics $Y_{\ell m}$. One can then determine the size of the anisotropies as a function of ℓ , with larger ℓ corresponding to smaller angles, and hence smaller length scales. Current CMB observation probe this power spectrum down to (comoving) length scales of about one Mpc. These observations imply very small primordial density perturbations at such large length scales, characterized by the power $\mathcal{P}_{\mathcal{R}_c} \simeq 10^{-9}$.

However, it is possible that the primordial density perturbations become much larger at smaller length scales, beyond the range probed by cosmological observations. Indeed, it is conceivable that these perturbations are so large that overdense regions collapse to form Primordial Black Holes (PBHs) just after the end of inflation [1, 2, 3]. They are called “primordial” since they do not originate from the gravitational collapse of burnt-out stars; they could thus have any mass, including masses well below or well above stellar masses. Here we assume that the fluctuations which sourced the PBHs are also generated during inflation, specifically towards the end of inflation, well after the length scales probed by conventional cosmological observations exited the horizon.

There are various constraints on PBH formation. For example, the density of roughly stellar mass black holes has to satisfy limits from searches for microlensing. Very light black holes could have evaporated (via Hawking radiation) in the epoch of Big Bang nucleosynthesis, altering the predicted isotope abundances. These and other constraints have recently been compiled in [4]. They can be translated into upper limits on the amplitude of the power spectrum at the length scales relevant for PBH formation, typically $\mathcal{P}_{\mathcal{R}_c} < 10^{-2} - 10^{-1}$ with some scale dependence.

Clearly the power spectrum has to change dramatically towards the end of inflation for PBH formation to occur. In the framework of standard slow-roll inflation, this implies that the slow-roll parameters, and hence the inflaton potential, also should show large variations. One simple, and yet well motivated, model that can feature large variations of the slow-roll parameters is the running-mass model [5, 6], a type of inflationary model which emerges naturally in the context of supersymmetric extensions of the Standard Model. The model is of the single-field type, but nevertheless it has relatively strong scale-dependence (running) of the spectral index. Previous studies of this model [7] showed that it can indeed accommodate sufficiently large positive running of the spectral index to allow for PBH formation. However, the recent 7-year WMAP data [8] prefer *negative* running of the spectral index.

In this paper we therefore revisit the running mass model. We expand on refs.[7] by including the running of the running of the spectral index, which is only weakly constrained by existing CMB data. Similarly, we include the running of the running of the inflaton mass parameter in the potential. We show that for some (small) range of parameters, this model can still accommodate sufficiently large density perturbations near the end of inflation to allow for the formation of PBHs with mass larger than 10^{15} g, which are sufficiently long-lived to be candidates for Cold Dark Matter (CDM). As a by-product we show that even with the additional term in the potential, the model does not allow for significant *negative* running of the spectral index.

The remainder of this paper is organized as follows: In section 2 we briefly review the formalism of PBH formation. In section 3 we discuss the running-mass inflation model, including the running of the running of the mass. We compute the slow-roll parameters which allow us

to determine the spectral index, its running, and the running of the running. In section 4 we perform a numerical analysis where we compute the spectral index at PBH scales exactly, by numerically solving the equation of motion of the inflaton field. Finally, we conclude in section 5.

2 Formation of Primordial Black Holes

PBHs may have formed during the very early universe, and if so can have observational implications at the present epoch, e.g. from effects of their Hawking evaporation [1] for masses $\lesssim 10^{15}$ g, or by contributing to the present “cold” dark matter density if they are more massive than 10^{15} g [3]. (These PBHs would certainly be massive enough to be dynamically “cold”¹).

The traditional treatment of PBH formation is based on the Press-Schechter formalism [10] used widely in large-scale structure studies. Here the density field is smoothed on a scale $R(M)$. In the case at hand, $R(M)$ is given by the mass enclosed inside radius R when R crossed the horizon. The probability of PBH formation is then estimated by simply integrating the probability distribution $P(\delta; R)$ over the range of perturbations δ which allow PBH formation: $\delta_{\text{th}} < \delta < \delta_{\text{cut}}$, where the upper limit arises since very large perturbations would correspond to separate closed ‘baby’ universes [3, 11]. We will show that in practice $P(\delta; R)$ is such a rapidly decreasing function of δ above δ_{th} that the upper cutoff is not important. The threshold density is taken as $\delta_{\text{th}} > w$, where $w = p/\rho$ is the equation of state parameter describing the epoch during which PBH formation is supposed to have occurred [3]. Here we take $w = 1/3$, characteristic for the radiation dominated epoch which should have started soon after the end of inflaton. However the correct value of the threshold δ_{th} is quite uncertain. Niemeyer and Jedamzik [12] carried out numerical simulations of the collapse of the isolated regions and found the threshold for PBH formation to be 0.7. We will show that PBHs abundance is sensitive to the value of δ_{th} .

The fraction of the energy density of the Universe in which the density fluctuation exceeds the threshold for PBH formation when smoothed on scale $R(M)$, $\delta(M) > \delta_{\text{th}}$, which will hence end up in PBHs with mass $\geq \gamma M$,² is given as in Press-Schechter theory³

$$f(\geq M) = 2\gamma \int_{\delta_{\text{th}}}^{\infty} P(\delta; M(R)) d\delta. \quad (2.1)$$

Here $P(\delta; M(R))$ is the probability distribution function (PDF) of the linear density field δ smoothed on a scale R , and γ is the fraction of the total energy within a sphere of radius R that ends up inside the PBH.

¹It has been argued [9] that BH evaporation might leave a stable remnant with mass of order of the Planck mass, which could form CDM; we will not pursue this possibility here.

²Throughout we assume for simplicity that the PBH mass is a fixed fraction γ of the horizon mass corresponding to the smoothing scale. This is not strictly true. In general the mass of PBHs is expected to depend on the amplitude, size and shape of the perturbations [12, 13].

³We follow ref.[14] in including a factor of two on the right-hand side; this factor is not very important for delineating the inflationary model parameters allowing significant PBH formation. Moreover, we set δ_{cut} to infinity.

For Gaussian fluctuations, the probability distribution of the smoothed density field is given by⁴

$$P(\delta; R) = \frac{1}{\sqrt{2\pi}\sigma_\delta(R)} \exp\left(-\frac{\delta^2}{2\sigma_\delta^2(R)}\right). \quad (2.2)$$

This PDF is thus uniquely determined by the variance $\sigma_\delta(R)$ of δ , which is given by

$$\sigma_\delta^2(R) = \int_0^\infty W^2(kR) \mathcal{P}_\delta(k) \frac{dk}{k}. \quad (2.3)$$

In order to compute the variance, we therefore have to know the power spectrum of δ , $\mathcal{P}_\delta(k) \equiv k^3/(2\pi^2) \langle |\delta_k|^2 \rangle$, as well as the volume-normalized Fourier transform of the window function used to smooth δ , $W(kR)$.

It is not obvious what the correct smoothing function $W(kR)$ is; a top-hat function has often been used in the past, but we prefer to use a Gaussian window function⁵,

$$W(kR) = \exp\left(-\frac{k^2 R^2}{2}\right). \quad (2.4)$$

Finally, on comoving hypersurfaces there is a simple relation between the density perturbation δ and the curvature perturbation \mathcal{R}_c [16]:

$$\delta(k, t) = \frac{2(1+w)}{5+3w} \left(\frac{k}{aH}\right)^2 \mathcal{R}_c(k), \quad (2.5)$$

The density and curvature perturbation power spectra are therefore related by

$$\mathcal{P}_\delta(k, t) = \frac{4(1+w)^2}{(5+3w)^2} \left(\frac{k}{aH}\right)^4 \mathcal{P}_{\mathcal{R}_c}(k). \quad (2.6)$$

The mass fraction of the Universe that will collapse into PBHs can now be computed by inserting eqs.(2.6) and (2.4) into eq.(2.3) to determine the variance as function of R . This has to be used in eq.(2.2), which finally has to be inserted into eq.(2.1). Since we assume a Gaussian $P(\delta)$ in eq.(2.2), the integral in eq.(2.1) simply gives an error function.

In order to complete this calculation one needs to relate the mass M to the comoving smoothing scale R . The number density of PBHs formed during the reheating phase just after the end of inflation will be greatly diluted by the reheating itself. We therefore only consider PBHs which form during the radiation dominated era after reheating is (more or less) complete. The initial PBHs mass M_{PBH} is related to the particle horizon mass M by⁶

$$M_{\text{PBH}} = \gamma M = \frac{4\pi}{3} \gamma \rho H^{-3}, \quad (2.7)$$

when the scale enters the horizon, $R = (aH)^{-1}$. Here the coefficient γ , which already appeared in eq.(2.1), depends on the details of gravitational collapse. A simple analytical calculation

⁴This PDF is often written as $P(\delta(R))$. However, we think it is more transparent to consider P to be the PDF of δ , which is just an integration variable in eq.(2.1). Eq.(2.2) shows that the functional form of $P(\delta)$ depends on the parameter R , which in turn depends on the horizon mass M .

⁵Bringmann *et al.* [15] argued that a top-hat window function predicts a larger PBH abundance.

⁶Throughout the paper we put $c = \hbar = k_B = 1$.

suggest that $\gamma \simeq w^{3/2} \simeq 0.2$ during the radiation era [3]. During radiation domination $aH \propto a^{-1}$, and expansion at constant entropy gives $\rho \propto g_*^{-1/3} a^{-4}$ [17] (where g_* is the number of relativistic degrees of freedom, and we have approximated the temperature and entropy degrees of freedom as equal). This implies that

$$M_{\text{PBH}} = \gamma M_{\text{eq}} (k_{\text{eq}} R)^2 \left(\frac{g_{*,\text{eq}}}{g_*} \right)^{1/3}, \quad (2.8)$$

where the subscript ‘‘eq’’ refers to quantities evaluated at matter–radiation equality. In the early Universe, the effective relativistic degree of freedom g_* is expected to be of order 100, while $g_{*,\text{eq}} = 3.36$ and $k_{\text{eq}} = 0.07 \Omega_{\text{m}} h^2 \text{ Mpc}^{-1}$ ($\Omega_{\text{m}} h^2 = 0.1334$ [8]). The horizon mass at matter–radiation equality is given by

$$M_{\text{eq}} = \frac{4\pi}{3} \rho_{\text{rad,eq}} H_{\text{eq}}^{-3} = \frac{4\pi}{3} \frac{\rho_{\text{rad},0}}{k_{\text{eq}}^3 a_{\text{eq}}}, \quad (2.9)$$

where $a_{\text{eq}}^{-1} = (1 + z_{\text{eq}}) = 3146$ and (assuming three species of massless neutrinos) $\Omega_{\text{rad},0} h^2 = 4.17 \times 10^{-5}$. Then it is straightforward to show that

$$\frac{R}{1 \text{ Mpc}} = 5.54 \times 10^{-24} \gamma^{-\frac{1}{2}} \left(\frac{M_{\text{PBH}}}{1 \text{ g}} \right)^{1/2} \left(\frac{g_*}{3.36} \right)^{1/6}. \quad (2.10)$$

Note that $M_{\text{PBH}} \propto R^2$, not $\propto R^3$ as one might naively have expected. Recall that M_{PBH} is related to the horizon mass at the time when the comoving scale R again crossed into the horizon. Larger scales re–enter later, when the energy density was lower; this weakens the dependence of M_{PBH} on R . Moreover, the lightest black holes to form are those corresponding to a comoving scale that re–enters the horizon immediately after inflation.⁷

The Gaussian window function in eq.(2.3) strongly suppresses contributions with $k > 1/R$. At the same time, the factor k^4 in eq.(2.6) suppresses contributions to the integral in eq.(2.3) from small k . As a result, this integral is dominated by a limited range of k –values near $1/R$. Over this limited range one can to good approximation assume a power–law primordial power spectrum with *fixed* power n_S ⁸ $\mathcal{P}_{\mathcal{R}_c}(k) = \mathcal{P}_{\mathcal{R}_c}(k_R) (k/k_R)^{n_S(R)-1}$, with $k_R = 1/R$. With this ansatz, the variance of the primordial density field at horizon crossing is given by

$$\sigma_\delta^2(R) = \frac{2(1+w)^2}{(5+3w)^2} \mathcal{P}_{\mathcal{R}_c}(k_R) \Gamma[(n_S(R)+3)/2], \quad (2.11)$$

for $n_S(R) > -3$.

The power $\mathcal{P}_{\mathcal{R}_c}$ is known accurately at CMB scales; for example, $\mathcal{P}_{\mathcal{R}_c}(k_0) = (2.43 \pm 0.11) \times 10^{-9}$ at the ‘‘COBE scale’’ $k_0 = 0.002 \text{ Mpc}^{-1}$ [8]. In order to relate this to the scales relevant for PBH formation, we parameterize the power spectrum as

$$\mathcal{P}_{\mathcal{R}_c}(k_R) = \mathcal{P}_{\mathcal{R}_c}(k_0) (k_R/k_0)^{n(R)-1}. \quad (2.12)$$

⁷In fact, PBH formation might also occur on scales that never leave the horizon [18]. We do not consider this contribution here.

⁸‘‘Fixed’’ here means that n_S does not depend on k ; however, n_S does depend on R , since a large range of values of R has to be considered for PBH formation of different masses.

It is important to distinguish between $n_S(R)$ and $n(R)$ at this point. $n_S(R)$ describes the *slope* of the power spectrum at scales $k \sim k_R = 1/R$, whereas $n(R)$ fixes the *normalization* of the spectrum at $k_R \gg k_0$. The two powers are identical if the spectral index is strictly constant, i.e. if neither n_S nor n depend on R . However, in this case CMB data imply [8] that $n = n_S$ is close to unity. Eqs.(2.11) and (2.12) then give a very small variance, leading to essentially no PBH formation.

Significant PBH formation can therefore only occur in scenarios with running spectral index. We parameterize the scale dependence of n as [19]:

$$n(R) = n_S(k_0) - \frac{1}{2!} \alpha_S \ln(k_0 R) + \frac{1}{3!} \beta_S \ln^2(k_0 R) + \dots; \quad (2.13)$$

recall that we are interested in $R \ll 1/k_0$, i.e. $\ln(k_0 R) < 0$. The parameters α_S and β_S denote the running of the effective spectral index n_S and the running of the running, respectively:

$$\begin{aligned} n_S(k_0) &\equiv \left. \frac{d \ln \mathcal{P}_{\mathcal{R}_c}}{d \ln k} \right|_{k=k_0}, \\ \alpha_S(k_0) &\equiv \left. \frac{dn_S}{d \ln k} \right|_{k=k_0}, \\ \beta_S(k_0) &\equiv \left. \frac{d^2 n_S}{d \ln^2 k} \right|_{k=k_0}. \end{aligned} \quad (2.14)$$

Eq.(2.13) illustrates the difference between $n(R)$ and $n_S(R)$. The latter has an expansion similar to eq.(2.13), but with the usual Taylor–expansion coefficients, 1 in front of α_S and $1/2$ in front of β_S . One therefore has

$$n_S(R) = n(R) - \frac{1}{2} \alpha_S \ln(k_0 R) + \frac{1}{3} \beta_S \ln^2(k_0 R) + \dots \quad (2.15)$$

Setting $n_S(k_0) = 1$ for simplicity, eq.(2.15) implies $n_S(R) = 2n(R) - 1$ for $\beta_S = 0$, and $n_S(R) = 3n(R) - 2$ for $\alpha_S = 0$. We will compute the variance $\sigma(R)$, and hence the PBH fraction f , for these two relations; they represent extreme cases if neither α_S nor β_S is negative.

The result of this calculation is shown in figure 1. Here we have fixed $\gamma = 0.2$, and show results for two choices of the threshold δ_{th} and three choices of $n(R)$. We see that scenarios where $n(R) = 1.3$ (or smaller) are safe in the SM, because there is no model–independent limit on f for $M_{\text{PBH}} < 10^{10}$ g [4]. As noted earlier, PBHs contributing to Dark Matter today must have $M_{\text{PBH}} \gtrsim 10^{15}$ g; at this mass, they saturate the DM relic density if $f \simeq 5 \times 10^{-19}$.⁹ Figure 1 shows that this requires $n(R) \simeq 1.37$ (1.41) for $\delta_{\text{th}} = 0.3$ (0.7). The dependence on n_S is much milder.

Figure 1 also illustrates a serious problem that all scenarios that aim to explain the required CDM density in terms of post–inflationary PBH formation face. We just saw that this can happen only if the spectral index n increases significantly between the scales probed by the CMB and other cosmological observations and the scale $R \simeq 10^{-9}$ pc relevant for the formation of 10^{15} g PBHs. However, n must then *decrease* rapidly when going to slightly smaller

⁹Note that f describes the fraction of the energy density in PBHs at the time of their formation. Since they behave like matter at all times, their fractional contribution to the energy density increases during the radiation–dominated epoch, and stays essentially constant during the subsequent matter–dominated epoch.

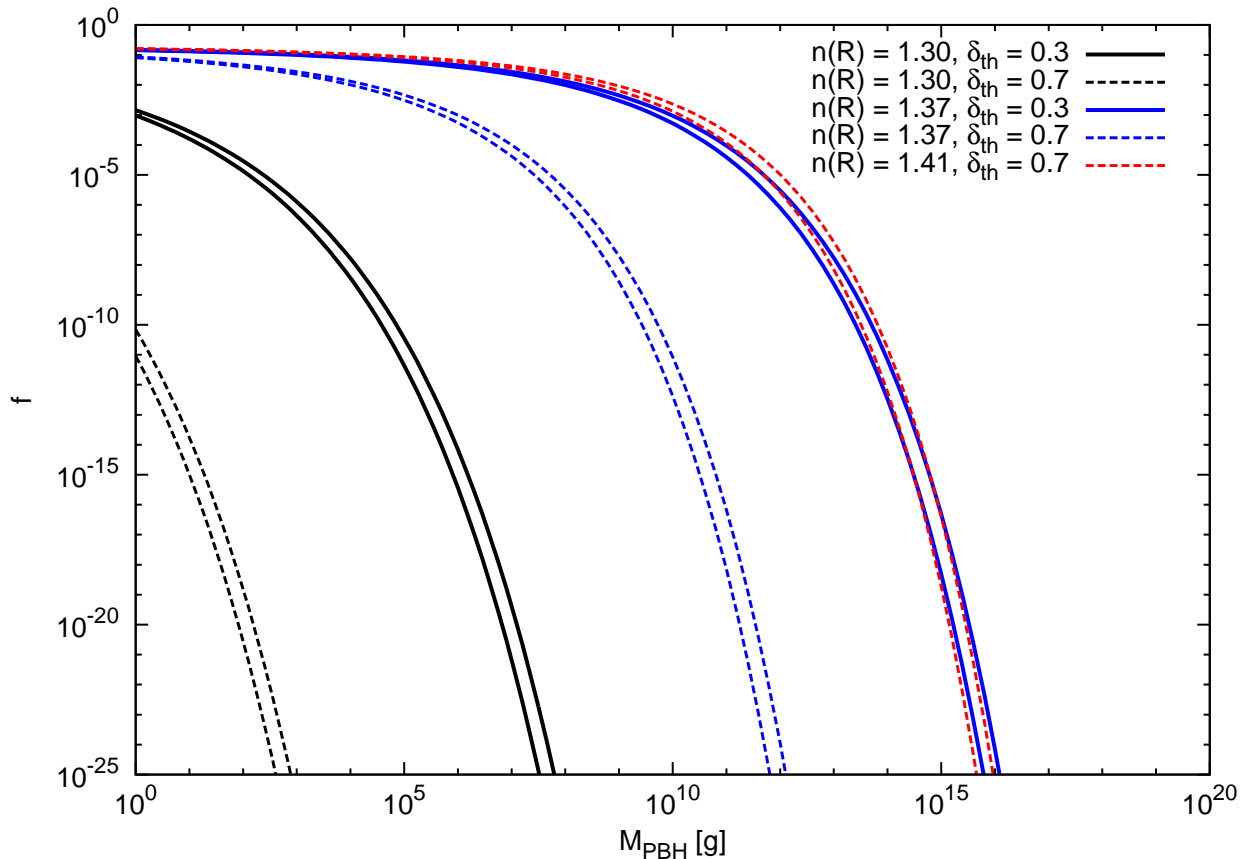


Figure 1: Fraction of the energy density of the universe collapsing into PBHs as a function of the PBH mass, for three different values of $n(R)$ and two different choices of the threshold $\delta_{\text{th}} = 0.3$ (0.7) for the solid (dashed) curves. On the upper [lower] of two curves with equal pattern and color we have assumed $n_S(R) = 2n(R) - 1$ [$n_S(R) = 3n(R) - 2$].

length scales, since otherwise one would *overproduce* lighter PBHs. For example, successful Big Bang Nucleosynthesis requires [4] $f(10^{13} \text{ g}) \leq 2 \times 10^{-20}$, about 12 orders of magnitude below that predicted by keeping $n(R)$ fixed at the value required for having 10^{15} g PBHs as CDM candidates. We will come back to this point at the end of our paper.

Another problem is that the expansion of $n(R)$ in eq.(2.13) will generally only be accurate if $|\ln(k_0 R)|$ is not too large. This is the case for cosmological observations, which probe scales $\gtrsim 1 \text{ Mpc}$. The expansion becomes questionable for the scales probed by PBH formation. For example, fixing $k_0 = 0.002 \text{ Mpc}^{-1}$, eq.(2.10) gives $|\ln(k_0 R)| = 41.1$ for $M_{\text{PBH}} = 10^{15} \text{ g}$. Fortunately within the framework of a given inflationary scenario this second problem can be solved by computing $n(R)$ and $n_S(R)$ exactly, rather than using the expansion (2.13).

Observational bounds on n_S and α_S can e.g. be found in ref.[8]. By requiring that these parameters remain within the 2σ ranges for all scales k between 10^{-4} Mpc^{-1} and 10 Mpc^{-1} , we find $\beta_S \lesssim 0.03$. Here we used the error bars derived from the analysis of WMAP7 data plus data on baryonic acoustic oscillations (BAO), ignoring possible tensor modes (as appropriate for small-field models), and including independent measurements of the Hubble constant as a prior (i.e. we used the “WMAP7+BAO+ H_0 ” data set). Here we use the pivot scale $k_0 =$

0.0155 Mpc^{-1} where $n_S(k_0)$ and $\alpha_S(k_0)$ are uncorrelated. On the other hand, eq.(2.13) shows that for $\alpha_S = 0$ we only need $\beta_S(k_0) \simeq 0.0016$ in order to generate sufficiently large density perturbations to allow formation of 10^{15} g PBHs. Even if we set $\alpha_S(k_0)$ equal to its central value, $\alpha_S(k_0) = -0.022$, we only need $\beta_S(k_0) \simeq 0.0032$. Including the running of the running of the spectral index thus easily allows to accommodate PBH formation in scenarios that reproduce all current cosmological observations at large scales.

Of course, this kind of model-independent analysis does not show whether simple, reasonably well-motivated inflationary models exist that can generate a sufficiently large β_S . One scenario that quite naturally accommodates strong scale dependence of the spectral index is the running-mass inflation model [5, 6]. We now apply our results to this model.

3 Running-Mass Inflation Model

This model, proposed by Stewart [5, 6], exploits the observation that in field theory the parameters of the Lagrangian are scale dependent. This is true in particular for the mass of the scalar inflaton, which can thus be considered to be a “running” parameter.¹⁰ The running of the mass parameter can be exploited to solve the “ η -problem” of inflation in supergravity [20]. This problem arises because the vacuum energy driving inflation also breaks supersymmetry. In “generic” supergravity models the vacuum energy therefore gives a large (gravity-mediated) contribution to the inflaton mass, yielding $|\eta| \sim 1$. However, this argument applies to the scale where SUSY breaking is felt, which should be close to the (reduced) Planck scale $M_P = 2.4 \times 10^{18}$ GeV. In the running mass model, renormalization group (RG) running of the inflaton mass reduces the inflaton mass, and hence $|\eta|$, at scales where inflation actually happens. There are four types of model, depending on the sign of the squared inflaton mass at the Planck scale, and on whether or not that sign change between M_P and the scales characteristic for inflation [21].

The simplest running-mass model is based on the inflationary potential

$$V_\phi = V_0 + \frac{1}{2}m_\phi^2(\phi)\phi^2, \quad (3.1)$$

where ϕ is a real scalar; in supersymmetry it could be the real or imaginary part of the scalar component of a chiral superfield. The natural size of $|m_\phi^2(M_P)|$ in supergravity is of order V_0/M_P^2 . Even for this large value of m_ϕ^2 , which gives $|\eta| \sim \mathcal{O}(1)$, the potential will be dominated by the constant term for $\phi^2 \ll M_P^2$; as mentioned above, running is supposed to reduce $|m_\phi^2|$ even more at lower ϕ^2 .

The potential (3.1) would lead to eternal inflation. One possibility to end inflation is to implement the idea of hybrid inflation [22]. To that end, one introduces a real scalar “waterfall field” ψ , and adds to the potential the terms¹¹

$$V_\psi = \frac{\lambda}{4}\phi^2\psi^2 - \sqrt{\frac{V_0\kappa}{6}}\psi^2 + \frac{\kappa}{24}\psi^4. \quad (3.2)$$

¹⁰Note that the physical, or pole, mass of the inflaton is not “running”; however, at the quantum level the physical mass differs from the parameter m_ϕ appearing in eq.(3.1) even if $\phi = 0$.

¹¹The parameters of this potential will in general also be scale dependent; however, this is immaterial for our argument.

Here λ and κ are real couplings, and the coefficient of the ψ^2 term has been chosen such that $V_{\text{inf}} = V_\phi + V_\psi$ has a minimum with $\langle V \rangle = 0$ if $\phi = 0$, $\psi \neq 0$. As long as $\phi^2 > \sqrt{\frac{8V_0\kappa}{3\lambda^2}}$, ψ remains frozen at the origin. Once ϕ^2 falls below this critical value, ψ quickly approaches its final vacuum expectation value, given by $\langle \psi \rangle^2 = \sqrt{\frac{24V_0}{\kappa}}$, while ϕ quickly goes to zero, thereby “shutting off” inflation. However, in this paper we focus on the inflationary period itself; the evolution of perturbations at length scales that left the horizon a few e-folds before the end of inflation should not be affected by the details of how inflation is brought to an end.¹²

During inflation, the potential is thus simply given by eq.(3.1). Here $m_\phi^2(\phi)$ is obtained by integrating an RG equation of the form

$$\frac{dm_\phi^2}{d \ln \phi} = \beta_m, \quad (3.3)$$

where β_m is the β -function of the inflaton mass parameter. If m_ϕ^2 is a pure SUSY-breaking term, to one loop β_m can be schematically written as [5, 24]

$$\beta_m = -\frac{2C}{\pi} \alpha \tilde{m}^2 + \frac{D}{16\pi^2} |\lambda_Y|^2 m_s^2, \quad (3.4)$$

where the first term arises from the gauge interaction with coupling α and the second term from the Yukawa interaction λ_Y . C and D are positive numbers of order one, which depend on the representations of the fields coupling to ϕ , \tilde{m} is a gaugino mass parameter, while m_s^2 is the scalar SUSY breaking mass-squared of the scalar particles interacting with the inflaton via Yukawa interaction λ_Y .

For successful inflation the running of m_ϕ^2 must be sufficiently strong to generate a local extremum of the potential V_ϕ for some nonvanishing field value, which we call ϕ_* . The inflaton potential will obviously be flat near ϕ_* , so that inflation usually occurs at field values not very far from ϕ_* . We therefore expand $m_\phi^2(\phi)$ around $\phi = \phi_*$. The potential we work with thus reads:

$$V = V_0 + \frac{1}{2} m_\phi^2(\phi_*) \phi^2 + \frac{1}{2} c \phi^2 \ln \left(\frac{\phi}{\phi_*} \right) + \frac{1}{4} g \phi^2 \ln^2 \left(\frac{\phi}{\phi_*} \right). \quad (3.5)$$

Here $c \equiv \left. \frac{dm_\phi^2}{d \ln \phi} \right|_{\phi=\phi_*}$ is given by the β -function of eq.(3.4), and $g \equiv \left. \frac{d^2 m_\phi^2}{d(\ln \phi)^2} \right|_{\phi=\phi_*}$ is given by the scale dependence of the parameters appearing in eq.(3.4). In contrast to earlier analyses of this model [21, 24, 25], we include the $\ln^2(\phi/\phi_*)$ term in the potential. This is a two-loop correction, but it can be computed by “iterating” the one-loop correction.¹³ Since the coefficient g of this term is of fourth order in couplings, one will naturally expect $|g| \ll |c|$. However, this need not be true if $|c|$ “happens” to be suppressed by a cancellation in eq.(3.4). Including the second correction to $m_\phi^2(\phi)$ seems natural given that we also expanded the running of the spectral index to second (quadratic) order.

Recall that we had defined ϕ_* to be a local extremum of V_ϕ , i.e. $V'(\phi_*) = 0$. This implies [21] $m_*^2 \equiv m_\phi^2(\phi_*) = -\frac{1}{2}c$; this relation is not affected by the two-loop correction $\propto g$.

¹²It has recently been pointed out that the waterfall phase might contribute to PBH formation [23].

¹³There are also “genuine” two-loop corrections, which can not be obtained from a one-loop calculation, but they only affect the term linear in $\ln(\phi/\phi_*)$. They are thus formally included in our coefficient c .

In order to calculate the spectral parameters n_S , α_S and β_S defined in eqs.(2.14), we need the first four slow-roll parameters, defined as [16]:¹⁴

$$\begin{aligned}\epsilon &\equiv \frac{M_{\text{P}}^2}{2} \left(\frac{V'}{V} \right)^2, \\ \eta &\equiv M_{\text{P}}^2 \frac{V''}{V}, \\ \xi^2 &\equiv M_{\text{P}}^4 \frac{V'V'''}{V^2}, \\ \sigma^3 &\equiv M_{\text{P}}^6 \frac{V'^2V''''}{V^3}.\end{aligned}\tag{3.6}$$

where primes denote derivatives with respect to ϕ . All these parameters are in general scale-dependent, i.e. they have to be evaluated at the value of ϕ that the inflaton field had when the scale k crossed out of the horizon. The spectral parameters are related to these slow-roll parameters by [16]:

$$\begin{aligned}n_S &= 1 - 6\epsilon + 2\eta, \\ \alpha_S &= -24\epsilon^2 + 16\epsilon\eta - 2\xi^2, \\ \beta_S &= -192\epsilon^3 + 192\epsilon^2\eta - 32\epsilon\eta^2 - 24\epsilon\xi^2 + 2\eta\xi^2 + 2\sigma^3.\end{aligned}\tag{3.7}$$

Slow-roll inflation requires $|\epsilon|, |\eta| \ll 1$. Combining eqs.(3.5) and (3.6) we see that we need $V_0 \gg c\phi^2L, g\phi^2L^2$, where we have introduced the short-hand notation

$$L \equiv \ln \frac{\phi}{\phi_*}.\tag{3.8}$$

In other words, the inflaton potential has to be dominated by the constant term, as noted earlier. Eqs.(3.6) then imply two strong inequalities between (combinations of) slow-roll parameters:

$$\begin{aligned}|\epsilon| &\ll |\eta|; \\ |\epsilon\eta| &\ll |\xi^2|.\end{aligned}\tag{3.9}$$

The first relation means that $n_S - 1$ is essentially determined by η . Similarly, both relations together imply that α_S is basically fixed by ξ^2 , while only the last two terms in the expression for β_S are relevant; these two terms are generically of similar order of magnitude. Finally, the factors of V appearing in the denominators of eqs.(3.6) can be replaced by V_0 . The spectral parameters are thus given by:

$$\begin{aligned}n_S - 1 &= 2\frac{cM_{\text{P}}^2}{V_0} \left[L + 1 + \frac{g}{2c} (L^2 + 3L + 1) \right]; \\ \alpha_S &= -2 \left(\frac{cM_{\text{P}}^2}{V_0} \right)^2 L \left[1 + \frac{g}{2c} (2L + 3) \right] \left[1 + \frac{g}{2c} (L + 1) \right]; \\ \beta_S &= 2 \left(\frac{cM_{\text{P}}^2}{V_0} \right)^3 L \left[1 + \frac{g}{2c} (L + 1) \right] \left[1 + \frac{g}{2c} (3L + 2) + \frac{g^2}{2c^2} \left(3L^2 + 5L + \frac{3}{2} \right) \right],\end{aligned}\tag{3.10}$$

¹⁴The powers on ξ^2 and σ^3 are purely by convention; in particular, ξ^2 could be negative.

where L has been defined in eq.(3.8). Clearly the spectral index is not scale–invariant unless c and g are very close to zero. Note that V_0 appears in eqs.(3.10) only in the dimensionless combination cM_{P}^2/V_0 , while ϕ only appears via L , i.e. only the ratio ϕ/ϕ_* appears in these equations.

In contrast, the absolute normalization of the power spectrum is given by (in slow–roll approximation)

$$\mathcal{P}_{\mathcal{R}_c} = \frac{1}{12\pi^2 M_{\text{P}}^6} \frac{V^3}{V'^2}. \quad (3.11)$$

This normalization is usually quoted at the ‘‘COBE scale’’ $k_0 = 0.002 \text{ Mpc}^{-1}$, where $\mathcal{P}_{\mathcal{R}} = 2.43 \times 10^{-9}$ [8]. Applying our potential (3.5) to eq.(3.11), replacing V by V_0 in the numerator, we see that $\mathcal{P}_{\mathcal{R}_c}$ not only depends on cM_{P}^2/V_0 and L , but also on the ratio $V_0/(M_{\text{P}}^2\phi^2)$. We can thus always find parameters that give the correct normalization of the power spectrum, for all possible combinations of the spectral parameters.

We want to find out whether the potential (3.5) can accommodate sufficient running of n_S to allow PBH formation. There are strong observational constraints on n_S and α_S . It is therefore preferable to use these physical quantities directly as inputs, rather than the model parameters cM_{P}^2/V_0 , L and g/c . To this end we rewrite the first eq.(3.10) as:

$$\frac{cM_{\text{P}}^2}{V_0} = \frac{n_S - 1}{2(L + 1) + \frac{g}{c}(L^2 + 3L + 1)}. \quad (3.12)$$

Inserting this into the second eq.(3.10) gives:

$$\alpha_S = -\frac{(n_S - 1)^2}{2} L \frac{[1 + \frac{g}{2c}(2L + 3)][1 + \frac{g}{2c}(L + 1)]}{[L + 1 + \frac{g}{2c}(L^2 + 3L + 1)]^2}. \quad (3.13)$$

We thus see that the running of the spectral index is ‘‘generically’’ of order $(n_S - 1)^2$; similarly, the running of the running can easily be seen to be $\propto (n_S - 1)^3$. This is true in nearly all inflationary scenarios that have a scale–dependent spectral index.

Eq.(3.13) can be solved for g/c . Bringing the denominator to the left–hand side leads to a quadratic equation, which has two solutions. They can be written as:

$$\frac{g}{2c} = -\frac{(L + 1)(L^2 + 3L + 1) + r_S L(1.5L + 2) \pm L\sqrt{r_S [(L + 1)^2 + 1] + r_S^2 (0.5L + 1)^2}}{(L^2 + 3L + 1)^2 + r_S L(2L + 3)(L + 1)}, \quad (3.14)$$

where we have introduced the quantity

$$r_S \equiv \frac{(n_S - 1)^2}{2\alpha_S}. \quad (3.15)$$

Since g and c are real quantities, eq.(3.14) only makes sense if the argument of the square root is non–negative. Note that the coefficients multiplying r_S and r_S^2 inside the square root are both non–negative. This means that the model can in principle accommodate any non–negative value of r_S . However, small negative values of r_S cannot be realized. It is easy to see that the constraint on r_S is weakest for $L = 0$. The argument of the square root is then positive if

$2r_S + r_S^2 > 0$, which implies either $r_S > 0$ or $r_S < -2$. Recalling the definition (3.15) we are thus led to the conclusion

$$\alpha_S \geq -\frac{(n_S - 1)^2}{4}; \quad (3.16)$$

this bound should hold on all scales, as long as the potential is described by eq.(3.5). Note that it is identical to the bound found in ref.[25], i.e. it is not affected by adding the term $\propto L^2$ to the inflaton potential. This is somewhat disappointing, since recent data indicate that α_S is negative at CMB scales. Even the generalized version of the running mass model therefore cannot reproduce the current 1σ range of α_S .

However, at the 2σ level significantly positive α_S values are still allowed. Let us therefore continue with our analysis, and search for combinations of parameters within the current 2σ range that might lead to significant PBH formation. Using eqs.(3.12) and (3.14) we can use $n_S(k_0) - 1$, $\alpha_S(k_0)$ and $L_0 \equiv \ln(\phi_0/\phi_*)$ as input parameters in the last eq.(3.10) to evaluate $\beta_S(k_0)$. This can then be inserted into eq.(2.13) to see how large the density perturbations at potential PBH scales are.

This numerical analysis is most easily performed at the ‘‘pivot scale’’, where the errors on n_S and α_S are essentially uncorrelated; at k -values above (below) this scale, n_S and α_S are correlated (anticorrelated) [26]. The pivot scale for the ‘‘WMAP7+BAO+ H_0 ’’ data set we are using is $k_0 \equiv k_{\text{pivot}} = 0.0155 \text{ Mpc}^{-1}$ [8].¹⁵ At this scale, observations give [8]:

$$\begin{aligned} n_S(k_0) &= 0.964 \pm 0.013; \\ \alpha_S(k_0) &= -0.022 \pm 0.020. \end{aligned} \quad (3.17)$$

We saw above that requiring the correct normalization of the power spectrum at CMB scales does not impose any constraint on the spectral parameters. However, the model also has to satisfy several consistency conditions. To begin with, it should provide a sufficient amount of inflation. In the slow-roll approximation, the number of e-folds of inflation following from the potential (3.5) is given by:

$$\begin{aligned} \Delta N(L) &= -\frac{2}{\tilde{c}} \int_{L_0}^L \frac{dL'}{L' \left[1 + \frac{g}{2c}(L' + 1)\right]} \\ &= -\frac{2}{\tilde{c} \left(1 + \frac{g}{2c}\right)} \left[\ln \frac{L}{L_0} - \ln \frac{1 + \frac{g}{2c}(L + 1)}{1 + \frac{g}{2c}(L_0 + 1)} \right], \end{aligned} \quad (3.18)$$

where we have introduced the dimensionless quantity

$$\tilde{c} \equiv \frac{2cM_{\text{P}}^2}{V_0}; \quad (3.19)$$

recall that it can be traded for $n_S(k_0) - 1$ using eq.(3.12). Moreover, $L \equiv \ln(\phi/\phi_*)$ can be related to the scale k through

$$k(L) = k_0 e^{\Delta N(L)}. \quad (3.20)$$

¹⁵This is the smaller of two k_{pivot} values given in ref.[8]. The difference between these two values is not important for our numerical analysis.

This can be inverted to give

$$L(k) = L_0 \frac{E(k) \left(1 + \frac{g}{2c}\right)}{1 + \frac{g}{2c} [L_0 (1 - E(k)) + 1]}, \quad (3.21)$$

where we have introduced

$$E(k) = \left(\frac{k}{k_0}\right)^{-\frac{\tilde{c}}{2}\left(1 + \frac{g}{2c}\right)}. \quad (3.22)$$

The problem is that the denominator in eq.(3.21) vanishes for some finite value of k . This defines an extremal value of ΔN :

$$\Delta N_{\text{ex}} = -\frac{2}{\tilde{c} \left(1 + \frac{g}{2c}\right)} \ln \left[1 + \frac{1}{L_0} \left(1 + \frac{2c}{g}\right)\right]. \quad (3.23)$$

A negative value of ΔN_{ex} is generally not problematic, since only a few e-folds of inflation have to have occurred before our pivot scale k_0 crossed out of the horizon. However, a small positive value of ΔN_{ex} would imply insufficient amount of inflation after the scale k_0 crossed the horizon. In our numerical work we therefore exclude scenarios with $-5 < \Delta N_{\text{ex}} < 50$, i.e. we (rather conservatively) demand that at least 50 e-folds of inflation can occur after k_0 crossed out of the horizon.

A second consistency condition we impose is that $|L|$ should not become too large. Specifically, we require $|L(k)| < 20$ for all scales between k_0 and the PBH scale. For (much) larger values of $|L|$ our potential (3.5) may no longer be appropriate, i.e. higher powers of L may need to be included.

Note that eq.(3.21) allows to compute the effective spectral index $n_S(k)$ *exactly*:

$$n_S(k) - 1 = [n_S(k_0) - 1] \frac{L(k) + 1 + \frac{g}{2c} [L(k)^2 + 3L(k) + 1]}{L_0 + 1 + \frac{g}{2c} (L_0^2 + 3L_0 + 1)}. \quad (3.24)$$

This in turn allows an *exact* (numerical) calculation of the spectral index $n(k)$:

$$n(k) - 1 = \frac{1}{\ln \frac{k}{k_0}} \int_0^{\ln \frac{k}{k_0}} [n_S(k') - 1] d \ln k'. \quad (3.25)$$

In our numerical scans of parameter space we noticed that frequently the exact value for $n(k)$ at PBH scales differs significantly from the values predicted by the expansion of eq.(2.13); similar statements apply to $n_S(k)$. This is not very surprising, given that $|\ln(k_0 R)| = 39.1$ for our value of the pivot scale and $M_{\text{PBH}} = 10^{15} \text{g}$. In fact, we noticed that even if $\alpha_S(k_0)$ and $\beta_S(k_0)$ are both positive, $n_S(k)$ may not grow monotonically with increasing k . In some cases $n_S(k)$ computed according to eq.(3.24) even becomes quite large at values of k some 5 or 10 e-folds below the PBH scale. This is problematic, since our calculation is based on the slow-roll approximation, which no longer works if $n_S - 1$ becomes too large. We therefore demanded $n_S(k) < 2$ for all scales up to the PBH scale; the first eq.(3.7) shows that this corresponds to $\eta < 0.5$. This last requirement turns out to be the most constraining one when looking for combinations of parameters that give large $n(k_{\text{PBH}})$.

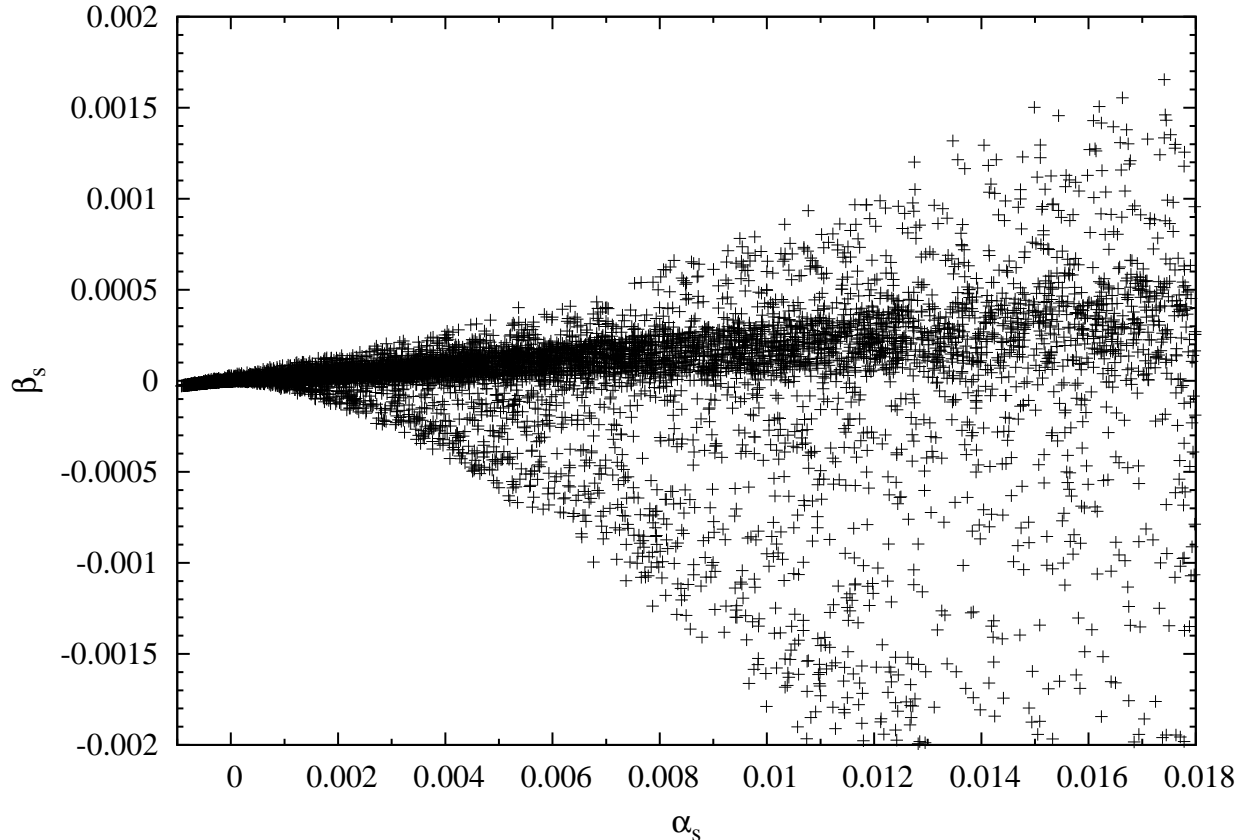


Figure 2: Scatter plot of $\beta_S(k_0)$ vs. $\alpha_S(k_0)$. Here the model parameters $\tilde{c} \equiv 2cM_P^2/V_0$, g/c and L_0 are scanned randomly, with flat probability distribution functions.

4 Numerical Results

We are now ready to present some numerical results. We begin in figure 2, which shows a scatter plot of the spectral parameters $\alpha_S(k_0)$ and $\beta_S(k_0)$, which has been obtained by randomly choosing model parameters \tilde{c} [defined in eq.(3.19)], g/c and L_0 in the ranges¹⁶ $|\tilde{c}| \leq 1$, $|g|M_P^2/V_0 \leq 1$, $|L_0| \leq 20$. We require that $n_S(k_0)$ and $\alpha_S(k_0)$ lie within their 2σ ranges, and impose the consistency conditions discussed above. The plot shows a very strong correlation between β_S and α_S : if the latter is negative or small, the former is also small in magnitude. Moreover, there are few points at large α_S , and even there most allowed combinations of parameters lead to very small β_S . The accumulation of points at small α_S can be understood from our earlier result (3.13), which showed that α_S is naturally of order $(n_S - 1)^2 < 0.004$ within 2σ . Moreover, β_S is naturally of order $\alpha_S^{3/2}$. On the other hand, for α_S values close to the upper end of the current 2σ range, we do find some scenarios where β_S is sufficiently large to allow the formation of 10^{15} g PBHs.

We also explored the correlation between $n_S(k_0)$ and $\alpha_S(k_0)$ (not shown). Here the only notable feature is the lower bound (3.16) on $\alpha_S(k_0)$; values of $\alpha_S(k_0)$ up to (and well beyond)

¹⁶We actually only find acceptable solutions for $|\tilde{c}| < 0.8$.

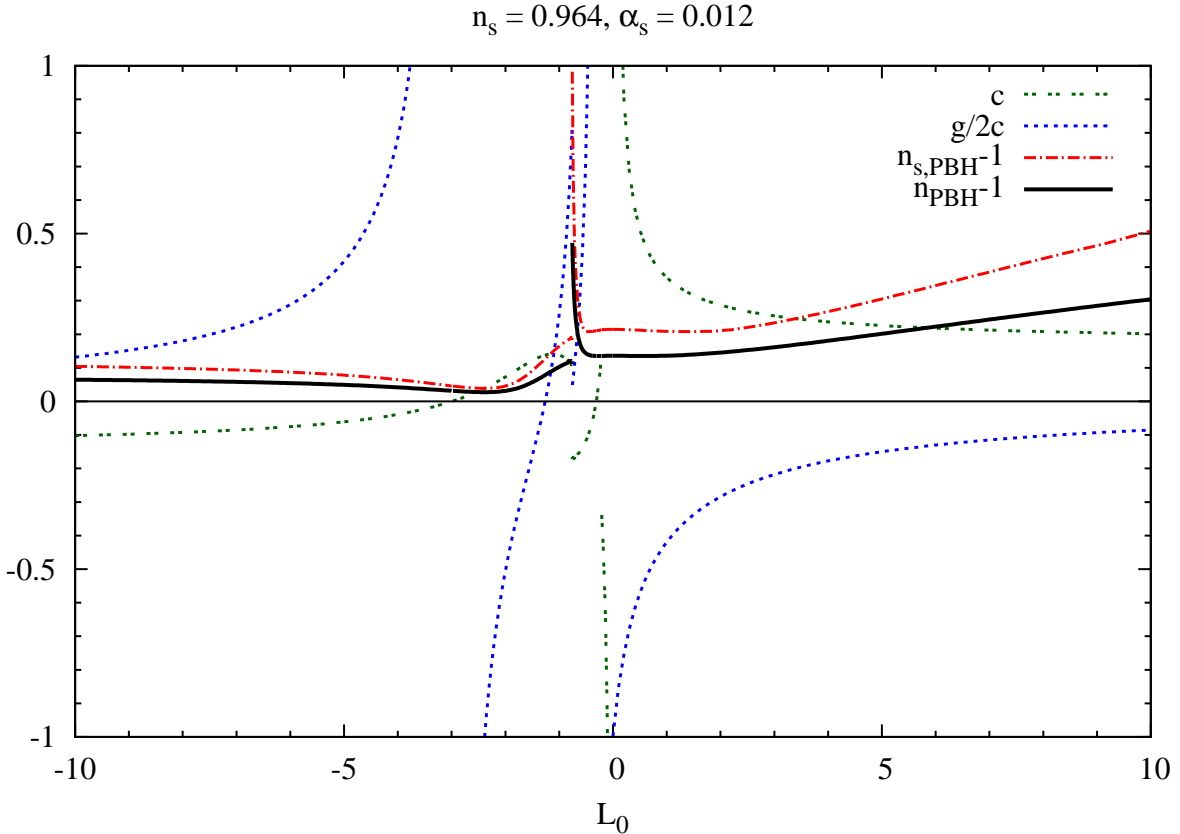


Figure 3: The potential parameters c (in units of $V_0/(2M_{\text{P}}^2)$; double-dotted [green] curve), $g/(2c)$ (dotted, blue), the effective spectral index $n_s - 1$ at the PBH scale (dot-dashed, red) and the spectral index $n - 1$ at the PBH scale (solid, black) are shown as functions of $L_0 = \ln(\phi_0/\phi_*)$, for $n_s(k_0) = 0.964$ and $\alpha_s(k_0) = 0.012$. If both solutions in eq.(3.14) for g/c are acceptable, we have taken the one giving larger n at the PBH scale.

its observational upper bound can be realized in this model for any value of $n_s(k_0)$ within the presently allowed range. Similarly, we do not find any correlation between $n_s(k_0)$ and $\beta_S(k_0)$. This lack of correlation can be explained through the denominator in eq.(3.13), which also appears (to the third power) in the expression for β_S once eq.(3.12) has been used to trade c for $n_s - 1$: this denominator can be made small through a cancellation, allowing sizable α_S even if n_s is very close to 1. Since the same denominator appears (albeit with different power) in the expressions for α_S and β_S , it does not destroy the correlation between these two quantities discussed in the previous paragraph.

Figure 2 indicates that large values of n at the PBH scale can be achieved only if α_S at the CMB scale is positive and not too small. In figure 3 we therefore explore the dependence of the potential parameters, and of the spectral parameters at the PBH scale on L_0 , for $n_s(k_0) = 0.964$, $\alpha_s(k_0) = 0.012$. Note that varying L_0 also changes the parameters c and g (or g/c), see eqs.(3.12) and (3.14). The latter in general has two solutions; however, for most values of L_0 , only one of them leads to sufficient inflation while keeping $|L| < 20$; if both solutions

are allowed, we take the one giving a larger spectral index at the PBH scale, taken to be $1.5 \times 10^{15} \text{ Mpc}^{-1}$ corresponding to $M_{\text{PBH}} = 10^{15} \text{ g}$. Note that n_S and n at the PBH scale are calculated exactly, using eqs.(3.7) and (3.25). We find that the expansion (2.13) is frequently very unreliable, e.g. giving the wrong sign for $n - 1$ at the PBH scale for $L_0 < -1$.

Figure 3 shows that \tilde{c} is usually well below 1, as expected from the fact that $n_S - 1 \propto \tilde{c}$, see the first eq.(3.10). Moreover, in most of the parameter space eq.(3.14) implies $|g| < |c|$; recall that this is also expected, since g is a two-loop term. We find $|g| > |c|$ only if $|c|$ is small. In particular, the poles in $g/(2c)$ shown in figure 3 occur only where c vanishes; note that the spectral parameters remain smooth across these ‘‘poles’’.

There are a couple of real discontinuities in figure 3, where the curves switch between the two solutions of eq.(3.14). The first occurs at $L_0 \simeq -0.756$. For smaller values of L_0 , the solution giving the smaller $|g/c|$ violates our slow-roll condition $|n_S - 1| < 1$ at scales close to the PBH scale. For larger L_0 this condition is satisfied. Just above the discontinuity, where n_S is close to 2 at the PBH scale, we find the largest spectral index at the PBH scale, which is close to 0.47. Recall from figure 1 that this will generate sufficiently large density perturbations to allow the formation of PBHs with $M_{\text{PBH}} = 10^{15} \text{ g}$. However, the formation of PBHs with this mass is possible only for a narrow range of L_0 , roughly $-0.756 \leq L_0 \leq -0.739$.

At $L_0 = -0.31$, c goes through zero, giving a pole in g/c as discussed above. Then, at $L_0 = -0.214$, the second discontinuity occurs. Here the curves switch between the two solutions of eq.(3.14) simply because the second solution gives a larger spectral index at the PBH scale. Right at the discontinuity both solutions give the same spectral index, i.e. the curve depicting n_{PBH} remains continuous; however, \tilde{c} jumps from about 0.132 to -0.339 . The effective spectral index n_S at the PBH scale also shows a small discontinuity. Recall from our discussion of eq.(2.15) that n_S will generally be larger than n at the PBH scale, but the difference between the two depends on the model parameters.

For very small values of $|L_0|$, \tilde{c} becomes very large; this region of parameter space is therefore somewhat pathological. For sizably positive L_0 , n at the PBH scale increases slowly with increasing L_0 , while $|\tilde{c}|$ and $|g/c|$ both decrease. However, the spectral index at the PBH scale remains below the critical value for the formation of long-lived PBHs.

Note that L always maintains its sign during inflation, since $L = 0$ corresponds to a stationary point of the potential, which the (classical) inflaton trajectory cannot cross. For most of the parameter space shown in figure 3, $|L|$ decreases during inflation. If $L_0 < 0$ decreasing $|L|$ corresponds to $V'(\phi_0) < 0$, i.e. the inflaton rolls towards a minimum of the potential at $\phi = \phi_*$. For $L_0 > 0$ we instead have $V'(\phi_0) > 0$, i.e. the inflaton rolls away from a maximum of the potential.

In fact, this latter situation also describes the branch of figure 3 giving the largest spectral index at the PBH scale; since here $L_0 < 0$, $|L|$ increases during inflation on this branch. This is illustrated in figures 4, which show the (rescaled) inflaton potential as well as the effective spectral index as function of either the inflaton field (left frame) or of the scale k (right frame). Note that all quantities shown here are dimensionless, and are determined uniquely by the dimensionless parameters \tilde{c} defined in eq.(3.19), g/c and L_0 . This leaves two dimensionful quantities undetermined, e.g. V_0 and ϕ_* ; one combination of these quantities can be fixed via the normalization of the CMB power spectrum, leaving one parameter undetermined (and irrelevant for our discussion).

The left frame shows that the (inverse) scale k first increases quickly as ϕ rolls down from

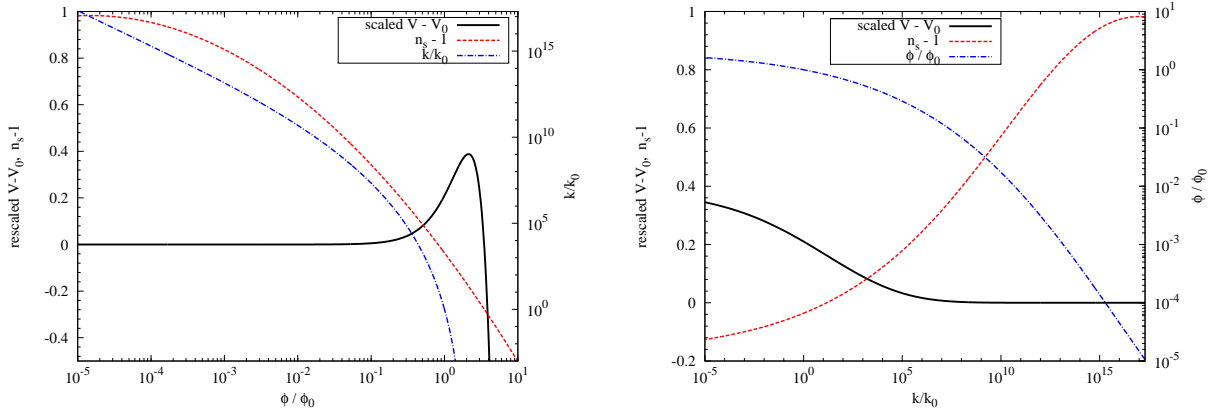


Figure 4: Evolution of the rescaled inflaton potential, $4M_{\text{P}}^2(V - V_0)/(V_0\phi_0^2)$ (solid, black), and of the effective spectral index n_S (dashed, red), as a function of the inflaton field ϕ/ϕ_0 (left frame) or of the ratio of scales k/k_0 (right frame). In the left frame the dot-dashed (blue) curve shows k/k_0 , whereas in the right frame it depicts ϕ/ϕ_0 ; this curve in both cases refers to the scale to the right. We took $\tilde{c} = -0.1711$, $g/c = 0.09648$, $L_0 = -0.756$; these parameters maximize the spectral index at the PBH scale for $n_S(k_0) = 0.964$, $\alpha_S(k_0) = 0.012$ (see figure 3).

its initial value ϕ_0 . This means that ϕ initially moves rather slowly, as can also be seen in the right frame. Since $\alpha_S > 0$, the effective spectral index increases with increasing k . The right frame shows that this evolution is quite nonlinear, although for $k/k_0 \lesssim 10^{10}$, $n_S(k)$ is to good approximation a parabolic function of $\ln(k/k_0)$. However, for even smaller scales, i.e. larger k , the rate of growth of n_S decreases again, such that $n_S - 1$ reaches a value very close to 1 at the scale $k = 1.6 \times 10^{16} k_0$ relevant for the formation of PBHs with $M_{\text{PBH}} = 10^{15}$ g. Recall that we only allow solutions where $n_S(k) < 2$ for the entire range of k considered; figures 4 therefore illustrate our earlier statement that this constraint limits the size of the spectral index at PBH scales.

The left frame of figure 4 shows that the inflaton potential as written becomes unbounded from below for $\phi \rightarrow +\infty$. This can be cured by introducing a quartic (or higher) term in the inflaton potential; the coefficient of this term should be chosen sufficiently small not to affect the discussion at the values of ϕ of interest to us. Note also that this pathology of our inflaton potential is not visible in the right frame, since assuming $\phi = \phi_0 < \phi_*$ at $k = k_0$, the inflaton field can never have been larger than ϕ_* : as noted above, it cannot have moved across the maximum of the potential.

Figure 2 indicated a strong dependence of the maximal spectral index at PBH scales on $\alpha_S(k_0)$. This is confirmed by figure 5, which shows the maximal possible $n(k_{\text{PBH}})$ consistent with our constraints as function of $\alpha_S(k_0)$, as well as the corresponding values of the parameters \tilde{c} , g/c and L_0 . We saw in the discussion of eq.(3.14) that $\alpha_S < 0$ is only allowed for a narrow range of L_0 . In this very constrained corner of parameter space, $n(k_{\text{PBH}})$ remains less than 1, although the effective spectral index $n_S(k_{\text{PBH}})$ can exceed 1 for $\alpha_S(k_0) > -1.7 \times 10^{-4}$; recall that for the given choice $n_S(k_0) = 0.964$, solutions only exist if $\alpha_S(k_0) > -3.24 \times 10^{-4}$, see eq.(3.16).

For $\alpha_S(k_0) \leq 1.5 \times 10^{-4}$ the optimal set of parameters lies well inside the region of parameter space delineated by our constraints. $n_S(k_{\text{PBH}})$ therefore grows very fast with increasing $\alpha_S(k_0)$.

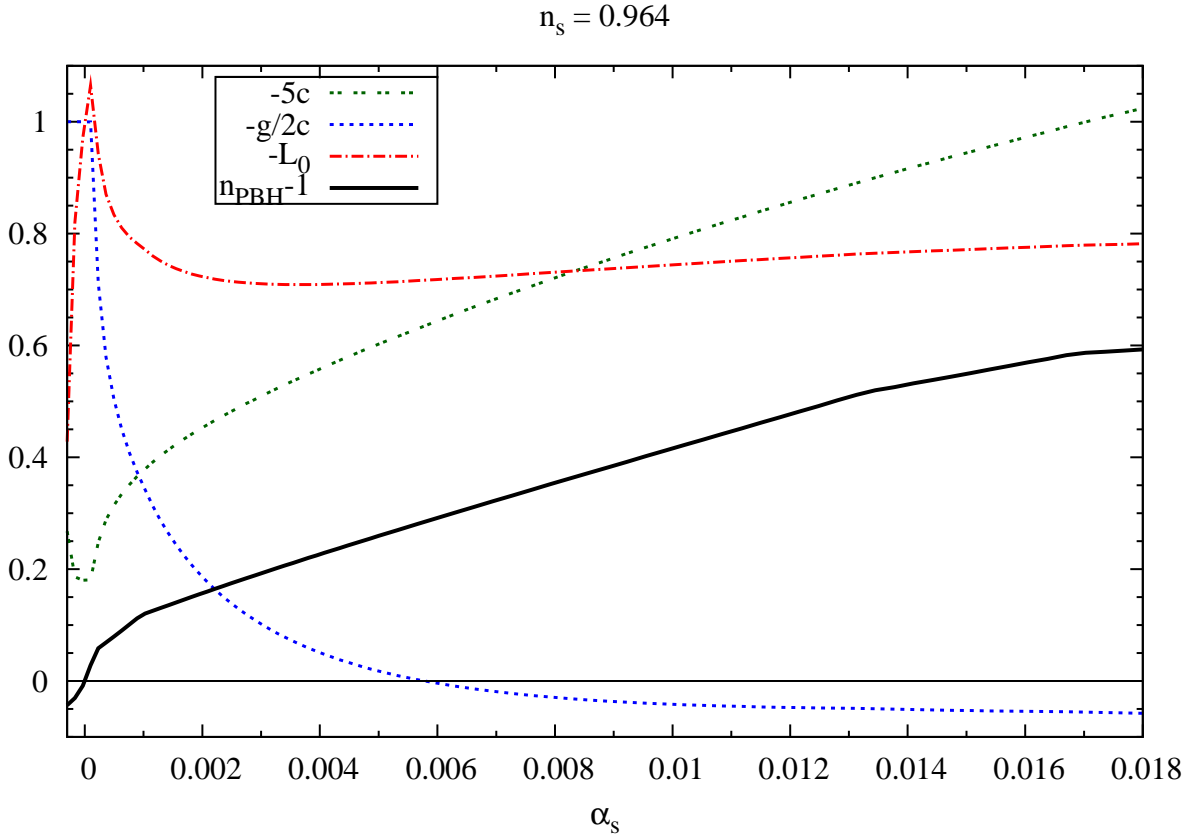


Figure 5: The solid (black) curve shows the maximal spectral index at the PBH scale $k_{\text{PBH}} = 1.6 \times 10^{19} k_0$ that is consistent with the constraints we impose, as function of $\alpha_S(k_0)$. The other curves show the corresponding model parameters: \tilde{c} (double-dotted, green), multiplied with -5 for ease of presentation; $-g/(2c)$ (dotted, blue); and $-L_0$ (dot-dashed, red). $n_S(k_0)$ is fixed at 0.964, but the bound on n_{PBH} is almost independent of this choice.

For these very small values of $\alpha_S(k_0)$, the largest spectral index at PBH scales is always found for $g = -2c$, which implies that the second derivative of the inflaton potential also vanishes at $\phi = \phi_*$, i.e. ϕ_* corresponds to a saddle point, rather than an extremum, of the potential.

For slightly larger values of $\alpha_S(k_0)$ the choice $g = -2c$ allows less than 50 e-folds of inflation after k_0 exited the horizon. Requiring at least 50 e-folds of inflation therefore leads to a kink in the curve for $n(k_{\text{PBH}})$. The optimal allowed parameter set now has considerable smaller $|g/c|$, but larger $|\tilde{c}|$.

The curve for the maximal $n(k_{\text{PBH}})$ shows a second kink at $\alpha_S(k_0) = 0.001$. To the right of this point the most important constraint is our requirement that $|n_S - 1| < 1$ at all scales up to k_{PBH} , as discussed in connection with figures 3 and 4. Note that for $\alpha_S(k_0) > 0.014$, the optimal parameter choice leads to n_S reaching its maximum at some intermediate k close to, but smaller than, k_{PBH} . This leads to a further flattening of the increase of $n(k_{\text{PBH}})$.

We nevertheless see that for values of $\alpha_S(k_0)$ close to the upper end of the 2σ range specified in (3.17) the spectral index at the scale relevant for the formation of 10^{15} g PBHs can be well above the minimum for PBH formation found in section 2. Figure 1 then implies that the

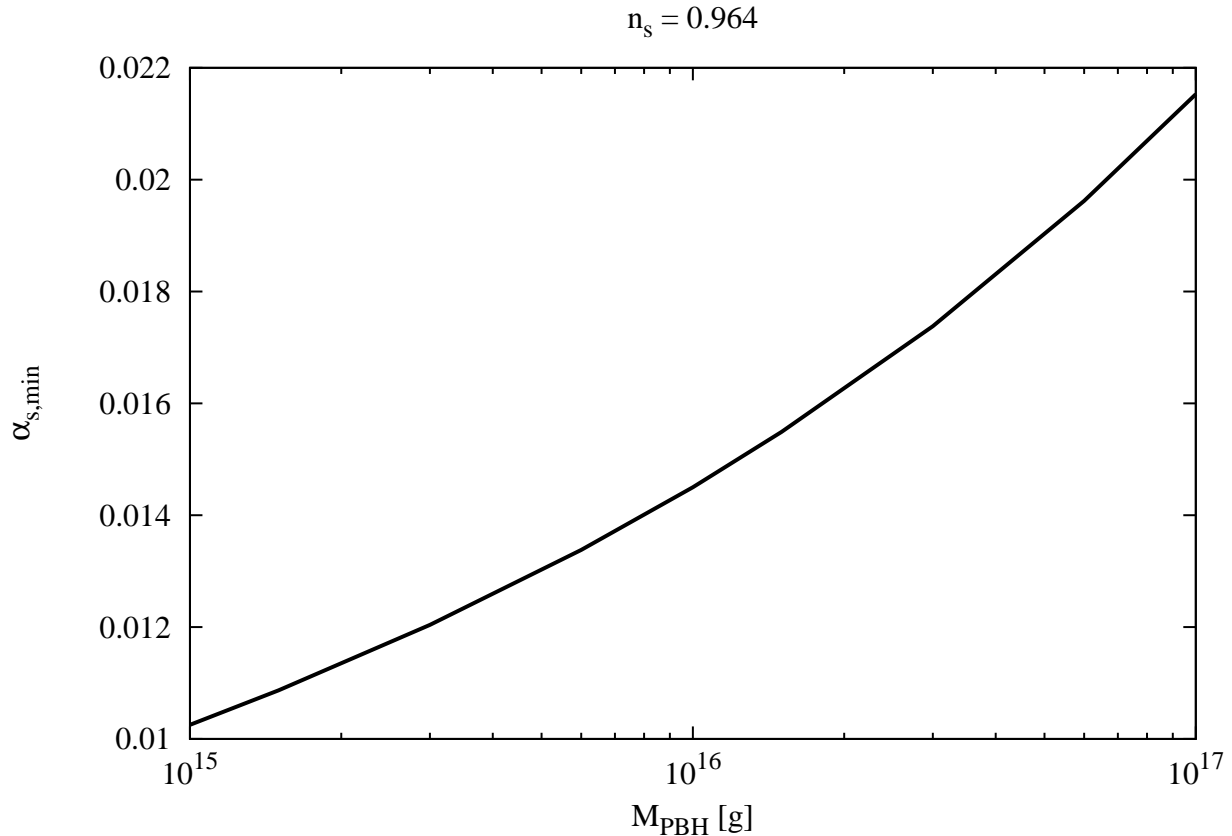


Figure 6: The minimal value of $\alpha_S(k_0)$ that allows the formation of primordial black holes of a given mass as a result of density perturbations produced during the slow-roll phase of inflation.

formation of considerably heavier PBHs might be possible in running mass inflation. However, larger PBH masses correspond to smaller k_{PBH} , see eq.(2.10). This in turn allows for less running of the spectral index. In order to check whether even heavier PBHs might be formed during the slow-roll phase of running mass inflation, one therefore has to re-optimize the parameters for different choices of k_{PBH} .

The result of such an analysis is shown in figure 6. We see that in the given model, the formation of PBHs that are sufficiently massive, and hence long-lived, to be CDM candidates could only have been triggered during the slow-roll phase of inflation if $\alpha_S(k_0)$ is more than one standard deviation above its central value. If $\alpha_S(k_0)$ is at the upper end of its present 2σ range, PBHs with mass up to 5×10^{16} g could have formed as result of density perturbations created at the end of slow-roll inflation. These results are again insensitive to the value of $n_S(k_0)$.

5 Summary and Conclusions

In this paper we have investigated the formation of primordial black holes in the radiation-dominated era just after inflation. We have focused on density perturbations originating from

the slow-roll phase of inflation. In section 2 we reviewed the Press–Schechter type formalism for PBH formation. We found that the formation of PBHs with mass larger than 10^{15} g, which could form (part of) the cold Dark Matter in the Universe, the spectral index at scale k_{PBH} should be at least 1.37, even for the lower value of $1/3$ for the threshold δ_{th} . This value is higher than the value 1.25 found in [27] because here we have assumed that the mass of the collapsed region to form PBH is only 20% of the entire energy density inside the particle horizon.

This spectral index is much above the value measured in the CMB. PBH formation therefore requires significant positive running of the spectral index when k is increased. In contrast, current observations favor a negative first derivative of the spectral index. For the central value $n_S(k_0) = 0.964$, where k_0 is the CMB pivot scale, the first derivative $\alpha_S(k_0)$ would need to exceed 0.020 if it alone were responsible for the required increase of the spectral index; this is outside the current 2σ range for this quantity. However, the second derivative (the “running of the running”) is currently only very weakly constrained. We showed in a model-independent analysis that this easily allows values of $n(k_{\text{PBH}})$ large enough for PBH formation, even if the first derivative of the spectral index is negative at CMB scales.

In section 3 we applied this formalism to the “running-mass” model of inflation, which had previously been shown to allow sufficiently large positive running of the spectral index to yield PBH formation. In contrast to previous analyses, we included a term quadratic in the logarithm of the field, i.e. we included the “running of the running” of the inflaton mass along with the “running of the running” of the spectral index. We showed that this model can accommodate a sizably positive second derivative of the spectral index at PBH scales. However, this is only possible if the first derivative is also positive and sizable. In fact, like most inflationary scenarios with a smooth potential [28] the model does not permit large negative running of the spectral index at CMB scales. Current data prefer negative running of the spectral index at CMB scales, but are consistent with sufficiently large positive running at the 2σ level. Moreover, we saw that a quadratic (in $\ln k$) extrapolation of the spectral index to PBH scales is not reliable, and therefore computed the spectral index exactly. Imposing several consistency conditions, we found that density perturbations that are sufficiently large to trigger PBH formation only occur for a very narrow region of parameter space. Among other things, the signs of the parameters of the inflaton potential must be chosen such that the potential has a local maximum, and the initial value of the field must be slightly (by typically less than one e-fold) below this maximum.

We emphasize that obtaining sufficiently large density perturbations at small scales is only a necessary condition for successful PBH formation. One major challenge of this model is that for parameters allowing PBH formation the spectral index keep increasing at yet smaller scales. Parameters that lead to the formation of many PBHs with mass around 10^{15} g, which could form the Dark Matter in the universe, would predict the over-production of unstable PBHs, in conflict with data e.g. from the non-observation of black hole evaporation and (for yet smaller masses) Big Bang Nucleosynthesis. This problem seems quite generic for this mechanism. One way to solve it might be to abruptly cut off inflation just after the scales relevant for the formation of the desired PBHs leave the horizon, which could e.g. be achieved by triggering the waterfall field in hybrid inflation. However, this is somewhat in conflict with the use of the slow-roll formalism of structure formation, which is usually assumed to require a few more e-folds of inflation after the scales of interest left the horizon. Moreover, a sharp end of inflation means that the visible universe only inflated by about 45 e-folds; this solves the horizon problems only if the reheat temperature was rather low [17].

We can therefore not state with confidence that formation of PBHs as Dark Matter candidates is possible in running-mass inflation; all we can say is that certain necessary conditions can be satisfied. Even that is possible only for a very limited range of parameters. This also means that constraints from the over-production of PBHs only rule out a small fraction of the otherwise allowed parameter space of this model.

Acknowledgments

This work is supported in part by the DFG Transregio TR33 “The Dark Universe”. EE thanks the Bonn–Cologne Graduate School for support, and the KIAS School of Physics for hospitality. MD thanks the particle theory group of the university of Hawaii at Manoa for hospitality while this work was completed.

References

- [1] S. W. Hawking, *Mon. Not. Roy. Astron. Soc.* **152** (1971) 75.
- [2] B. J. Carr and S. W. Hawking, *Mon. Not. Roy. Astron. Soc.* **168** (1974) 399.
- [3] B. J. Carr, *Astrophys. J.* **201** (1975) 1.
- [4] A. S. Josan, A. M. Green and K. A. Malik, *Phys. Rev.* **D79** (2009), 103520 [arXiv: 0903.3184]; B. Carr, K. Kohri, Y. Sendouda and J. Yokoyama, *Phys. Rev.* **D81** (2010) 104019 [arXiv: astro-ph/0912.5297].
- [5] E. D. Stewart, *Phys. Lett.* **B391** (1997) 34 [arXiv: hep-ph/9606241].
- [6] E. D. Stewart, *Phys. Rev.* **D56** (1997) 2019 [arXiv: hep-ph/9703232].
- [7] S. M. Leach, I. J. Grivell and A. R. Liddle, *Phys. Rev.* **D62** (2000) 043516 [arXiv: astro-ph/0004296]; K. Kohri, D. H. Lyth and A. Melchiorri, *JCAP* **0804** (2008) 038 [arXiv: hep-ph/0711.5006]; L. Alabidi and K. Kohri, *Phys. Rev.* **D80** (2009) 063511 2009 [arXiv: 0906.1398]; E. Bugaev, P. Klimai, *Phys. Rev.* **D79** (2009) 103511 [arXiv: 0812.4247].
- [8] E. Komatsu *et. al*, *Astrophys. J. Suppl.* **192** (2011) 18 [arXiv: astro-ph/1001.4538].
- [9] J. H. MacGibbon, *Nature* **320** (1987) 308; B. J. Carr, J. H. Gilbert and J. E. Lidsey, *Phys. Rev.* **D50** (1994) 4853 [arXiv: astro-ph/9405027]; J. D. Barrow, E. J. Copeland and A. R. Liddle, *Phys. Rev.* **D46** (1992) 645; A. Bonanno and M. Reuter, *Phys. Rev.* **D62** (2000) 043008 [arXiv: hep-th/0002196].
- [10] W. H. Press and P. Schechter, *Astrophys. J.* **187** (1974) 425.
- [11] S. W. Hawking, *Mon. Not. R. Astron. Soc.* **168** (1974) 399.
- [12] J. Niemeyer and K. Jedamzik, *Phys. Rev. Lett.* **80** (1998) 5481; *Phys. Rev.* **D59** (1999) 124013.

- [13] M. Shibata and M. Sasaki, *Phys. Rev.* **D60** (1999) 0842002 [arXiv: gr-qc/9905064]; J. C. Hidalgo and A. G. Polnarev, *Phys. Rev.* **D79** (2009) 044006 [arXiv: 0806.2752].
- [14] E. J. Copeland, A. R. Liddle, J. E. Lidsey and D. Wands, *Phys. Rev.* **D58** (1998) 063508 [arXiv: gr-qc/9803070].
- [15] T. Bringmann, C. Kiefer and D. Polarski, *Phys. Rev.* **D65** (2002) 024008 [arXiv: astro-ph/0109404]; *ibid.* **67** (2003) 024024.
- [16] A. R. Liddle and D. H. Lyth, *Cosmological Inflation and Large-Scale Structure*, Cambridge University Press, 2000; D. H. Lyth and A. R. Liddle, *The Primordial Density Perturbation*, Cambridge University Press, 2009; Q. Huang, *JCAP* **0611** (2006) 004 [arXiv: astro-ph/0610389].
- [17] E. W. Kolb and M. S. Turner, *The Early Universe*, Addison-Wesley, Redwood City, 1990.
- [18] D. H. Lyth, K. A. Malik, M. Sasaki and I. Zaballa, *JCAP* **0601** (2006) 011 [arXiv: astro-ph/0510647]; I. Zaballa, A. M. Green, K. A. Malik and M. Sasaki, *JCAP* **0703** (2007) 010 [arXiv: astro-ph/0612379].
- [19] A. Kosowsky and M. S. Turner, *Phys. Rev.* **D52** (1995) 1739; N. Düchting, *Phys. Rev.* **D70** (2004) 064015 [arXiv: astro-ph/0406260].
- [20] For a review, see D. Lyth and A. Riotto, *Phys. Rept.* **314** (1999) 1-146 [arXiv: hep-ph/9807278].
- [21] L. Covi and D. H. Lyth, *Phys. Rev.* **D59** (1999) 063515 [arXiv: hep-ph/9809562].
- [22] A. D. Linde, *Phys. Rev.* **D49** (1994) 748 [arXiv: astro-ph/9307002].
- [23] D. H. Lyth, arXiv: 1012.4617 [astro-ph.CO], and references therein.
- [24] L. Covi, *Phys. Rev.* **D60** (1999) 023513 [arXiv: hep-ph/9812232].
- [25] L. Covi, D. H. Lyth, A. Melchiorri and C. J. Odman, *Phys. Rev.* **D70** (2004) 123521 [arXiv: astro-ph/0408129].
- [26] M. Cortês, A. R. Liddle and P. Mukherjee, *Phys. Rev.* **D75** (2007) 083520 [arXiv: astro-ph/0702170].
- [27] A. M. Green and A. R. Liddle, *Phys. Rev.* **D56** (1997) 6166 [arXiv: astro-ph/9704251].
- [28] R. Easther and H. Peiris, *JCAP* **0609** (2006) 010 [arXiv: astro-ph/0604214].